Title

PapillArray: An Incipient Slip Sensor for Dexterous Robotic or Prosthetic Manipulation – Design and Prototype Validation

Authors and Affiliations

Heba Khamis[1], Raquel Izquierdo Albero[1,2], Matteo Salerno[1,3], Ahmad Shah Idil[1], Andrew Loizou[1], Stephen J. Redmond[1]

[1] Graduate School of Biomedical Engineering, UNSW Australia
[2] Escuela Técnica Superior de Ingenieros Industriales, Universidad Politécnica de Valencia
[3] Politecnico di Torino

Corresponding Author

Name: Heba Khamis

Email: heba.a.khamis@unsw.edu.au

Abstract

The major failing of robotic and prosthetic grippers in mimicking the dexterity of the human hand is thought to be a lack of adequate tactile sensing which provides feedback for grip control. The majority of existing tactile sensors focus on determining the contact forces; however, other tactile parameters, such as friction and the occurrence of incipient slip, are equally important for dexterous manipulation, particularly in unstructured environments. In this work, a design is presented for a grip security sensor – the PapillArray – which consists of an array of silicone pillars with different uncompressed heights. When the sensor is compressed, the tallest pillars in the centre are under greater normal stress and thus able to generate a greater friction force; this encourages the shorter outer pillars to slip first when a tangential force is applied. The incipient slip (as pillars slip independently) can be detected by measuring the deflection of the individual pillars, and continuous force/torque measurement is not strictly required. Each incipient slip event acts as a warning that the grip/normal force should be increased. A simple mathematical description of the principle of operation of one embodiment of the PapillArray with a single taller central pillar surrounded by eight shorter outer pillars (of equal height) is offered. A prototype of this embodiment is also presented and tested under different normal forces and frictional conditions. The deflection of the central pillar and a single outer pillar are determined by video recording and subsequent point-tracking methods. The outer pillar was observed to slip at a lower tangential force than the central pillar. From the simplified model, a prediction of the tangential-to-normal force ratio at the moment of slip of the central pillar was made. The R^2 value for a line of best fit for the predicted and measured ratio was 0.986 indicating an excellent fit, and the gradient of the line was 0.935, indicating that the predicted value is a slight underestimate of the coefficient of friction; this could be due to the assumption of unbending pillars. Both with and without continuous force monitoring, the PapillArray sensor can be used to improve dexterous manipulation in robotic and prosthetic grippers. This paper provides a proof -of-concept for this sensing approach; future papers will deal with the problem of instrumenting the pillar deflection by other means.

Keywords

Sensor; tactile; grip; slip; friction; grip security

1. Introduction

The human hand is capable of performing complex manipulations of objects with ease. It can detect valuable information about the object as well as the contact interface, which is believed to be the key to performing highly dexterous manipulation. Each fingertip contains on approximately 2,000 mechanoreceptors embedded in the glabrous (hairless) skin regions, which individually sense vibration, pressure and skin-stretch [1] and as a population can provide information about object shape [2], texture and even friction [3]. Although robotic and prosthetic gripper design continues to evolve to try to emulate the dexterity of the human hand, it is still far from achieving comparable performance. One major limitation of robotic and prosthetic grippers is the lack of adequate tactile sensing, which provides feedback for grip control.

The field of tactile sensing is an active one and aims to fill this gap; however, the majority of existing tactile sensors focus on determining the normal and tangential forces at the interface [4]. While these quantities are important, there are certainly other tactile parameters that are also important for dexterous manipulation. Two such parameters are the coefficient of static friction (μ_s) and the occurrence and extent of incipient slip.

The μ_s of the contact interface helps to determine the minimum grip (normal) force required to hold an object of a specific weight (tangential force). In certain grip poses, if the μ_s is accurately estimated and the tangential force can be measured, then the grip (normal) force can be adjusted to hold the object. There is a large volume of literature on methods of tactile sensing for grip force control which attempt to detect gross slip of an object and estimate μ_s during the slip in order to adjust the grip force to arrest the slip [5-7]. However, in this approach, the gripper may respond too slowly to prevent dropping the object, and these methods are not considered viable due to the high risk of dropping objects. Another approach has been to detect μ_s on contact, however, the literature does not contain many resoundingly successful examples of such sensors. One such example was presented by Maeno et al. [8], however, this sensor only appears to work for a limited range of μ_s, and does not appear to give a precise measure. A similar approach was taken by Nakamura et al. [9] with a sensing interface that appears more capable of undergoing independent movement at different locations; however, a complicated ultrasonic transduction method was used. More recently, Chen et al. [10] described a sensor with legs that slip or stick on contact depending on the angle made with the surface which could determine a range for the coefficient of static friction. These sensors also suffer from the inability to provide a continuous measurement of μ_s in the case of changing frictional conditions, and the need to continuously monitor normal and tangential forces during manipulation.

An alternative to measuring μ_s and continuously monitoring the normal and tangential forces at the contact interface is to detect incipient slip, and adjust grip force following the occurrence of such an event – such as the adaptive motor response of humans during precision grip [11]. Incipient slip is defined as a relative displacement taking place on a narrow region of the surface of the sensor, while total slip involves a relative displacement across the whole surface. A recent review of artificial slip sensing [12] qualitatively evaluated some 34 slip sensors with respect to power consumption, compliance, sensitivity to external noise, manufacturability, computational cost, and whether or not incipient slip could be detected (not just gross slip). The different transduction strategies for slip detection (displacement, microvibration, force, and thermal) were also evaluated with respect to robustness of incipient slip detection and rejection of noise, integrability of the sensor with a robotic finger, and simplicity of the manufacturing process. The conclusions of the review were that despite the multitude of slip sensors reported in the literature, there is still no dominant, well established technology, and the existing slip sensors do not meet all the requirements on which they were evaluated in the review [12].

There are various sensors in the literature for measuring incipient slip [13-30]. However, all of these overlook one or more important factors which make the detection of incipient slip practicable, such as the need to allow different regions of the gripper-object interface to move independently, and the

need to instrument relative displacement of regions of the contact area, rather than detecting the vibration/acceleration caused when incipient slip occurs (these transduction mechanisms are unlikely to be compatible with autonomous robotic manipulation). Perhaps the most successful of the incipient slip sensors is the GelSight sensor [29]. A transparent elastomer skin is patterned with dots whose movements are tracked using video. This allows the measurement of relative displacement of different regions of the contact area. Some limitations of this design are that the contiguous elastomer coating somewhat hinders relative movement of the contact area required to encourage incipient slip, and furthermore, the entire sensing surface is in a single plane which means there is no differential in normal stress and hence traction (i.e., maximum friction force).

In this work, a design is presented for a grip security sensor - the PapillArray sensor, which is so named due to its resemblance to papillae (small rounded protuberances) in the human finger pad - which detects incipient slip while the grip is still secured, enabling force modulation before total loss of grip is experienced. The design here addresses some of the shortcomings of previous incipient slip sensors, namely, it allows different regions of the gripper-object interface to move independently, and has a curved surface such that the pressure distribution on the contact area is not uniform, encouraging slip on the periphery first, where the local grip force (and hence traction) is smallest. A simple mathematical description of the principle of operation of one embodiment of the PapillArray is also offered and a prototype is presented and tested under different normal forces and frictional conditions.

2. Methods

2.1 Principle of operation

The PapillArray sensor consists of an array of silicone pillars with different unloaded heights. The difference in pillar heights accounts for a different normal force being experienced by each of the pillars when the sensor is pressed against a surface or object and each of the pillars is compressed to the same final height. When a tangential force is also applied, and assuming the pillars cannot bend, all of the pillars of the sensor experience the same tangential force. This means that the ratio of tangential-to-normal force experienced by each pillar is different, and therefore, assuming a constant μ_s across the surface, if the tangential force increases, the pillar under the lowest normal force (the shortest pillar when uncompressed) will slip first when the tangential-to-normal force ratio is greater than μ_s. In a PapillArray sensor with many pillars of different heights, as the tangential force increases further, the next shortest pillar will slip, followed by the next, and so on, until the tallest pillar slips.

When the pillars are loaded with a tangential force, they are deflected away from their unloaded positions. While a pillar is stuck (not slipping) and the tangential force increases, it deflects further and further. When the pillar slips, it no longer deflects any further, and the position remains constant.

By measuring the deflection of each of the pillars, the moment each pillar slips can be determined. Each incipient slip event acts as a warning that the grip/normal force should be increased to maintain the stable grip of an object. The rate at which warnings are signalled as well as the number of warnings could indicate the urgency with which corrective action is required as well as the magnitude of the corrective action.

Below, a simplified model as well as a prototype and its validation are described for one embodiment of the PapillArray sensor, which consists of a central pillar surrounded by eight shorter outer pillars of equal height.

2.2 A simplified mechanical model

In Figure 1, two pillars of one embodiment of the PapillArray sensor are shown – the central pillar, and a single outer pillar (there are eight such smaller outer pillars in the prototype presented later) –

illustrating the difference in pillar height and showing the forces acting on each pillar. In this example (and in the prototype described in the following section), a longer central pillar, with height l_C, is surrounded by eight shorter outer pillars, each with height l_O. A simplified model of the pillar behaviour of this embodiment of the PapillArray sensor follows. Note that this model does not consider the apparent shortening in the vertical height of pillars as they bend.

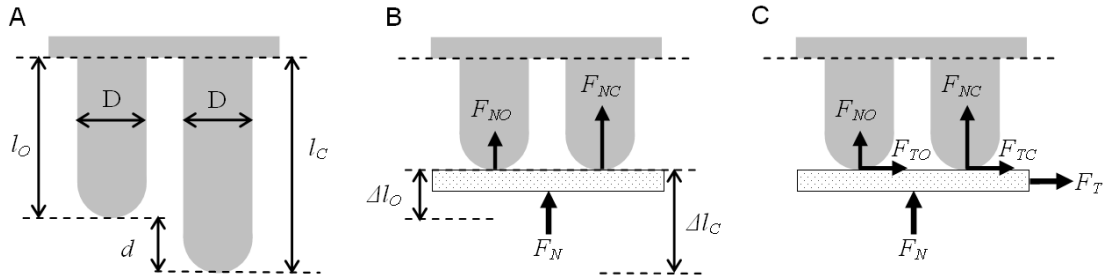

Figure 1. Illustration of a central pillar and outer pillar of a PapillArray sensor with nine pillars (one central pillar surrounded by eight outer pillars). Each pillar has a diameter D, and the central and outer pillars have uncompressed heights l_C and l_O, respectively. The sensor is shown when A) it is uncompressed, B) it is compressed with a flat surface, and C) the surface is sheared.

Figure 1A illustrates two pillars of an uncompressed PapillArray sensor. Each pillar has equal diameter, *D*, and different heights, l_C and l_O, respectively, where $d = l_C - l_O$. In Figure 1B, the sensor is pressed against a flat surface, such that both pillars are compressed to the same final height, resulting in a different normal (compression) force on each pillar – the pillar that was longer (when uncompressed) experiences a larger force (F_{NC}) than the pillar that was initially shorter (F_{NO}). We assume the material behaves as a linear elastic according to Hooke's Law. We also note that the gross normal force F_N is the sum of the normal forces acting on each pillar. In the case of a single central pillar, surrounded by eight outer pillars, this means:

$$F_{NC} = k\Delta l_C, \tag{1a}$$

$$F_{NO} = k\Delta l_O = k(\Delta l_C - d) = F_{NC} - kd, \text{ and} \tag{1b}$$

$$F_N = F_{NC} + 8F_{NO} = 9k\Delta l_C - 8kd, \tag{1c}$$

where k is the spring constant of the elastic material of the pillars. Therefore:

$$F_{NC} = \frac{F_N}{9} + \frac{8kd}{9}, \text{ and} \tag{2a}$$

$$F_{NO} = \frac{F_N}{9} - \frac{kd}{9}. \tag{2b}$$

When a tangential force is also applied to the sensor by shearing the surface that is in contact, each of the pillars also experiences a tangential force (see Figure 1C). When all pillars are stuck to the surface (not slipping), and assuming that (i) the compressive strain on the pillars is small relative to their height, (ii) the difference in height between the longer and shorter pillars is also small relative to height, and (iii) the pillars do not bend appreciably relative to their height, then they all experience approximately the same tangential force, and the sum of these tangential forces is equal to the gross tangential force, F_T. In the case of a single central pillar, surrounded by eight outer pillars, this means:

$$F_{TC} = F_{TO}, \text{ and} \tag{3a}$$

$$F_T = F_{TC} + 8F_{TO} = 9F_{TO}, \tag{3b}$$

where F_{TC} is the tangential force on the central pillar and F_{TO} is the tangential force on one of the outer pillars.

Because the outer pillars are under a smaller normal force, and μ_s is the same for each pillar, the outer pillars will slip at a smaller gross tangential force than the central pillar. The outer pillars will start to slip when:

$$F_{TO} > \mu_s F_{NO}. \quad (4)$$

This occurs when the gross tangential force is:

$$F_T^{SO} = 9F_{TO} > 9\mu_s F_{NO} = 9\mu_s \left(\frac{F_N^{SO}}{9} - \frac{kd}{9}\right) = \mu_s (F_N^{SO} - kd). \quad (5)$$

While the outer pillars are slipping and the central pillar is still stuck, the outer pillars are contributing a limited amount of tangential force to the gross tangential force, due to the coefficient of kinetic friction (μ_k):

$$F_{TO} = \mu_k F_{NO}, \quad (6a)$$

and the central pillar will start to slip when:

$$F_{TC} > \mu_s F_{NC}. \quad (6b)$$

This occurs when the gross tangential force is:

$$F_T^{sC} = F_{TC} + 8F_{TO} > \mu_s F_{NC} + 8\mu_k F_{NO} = \frac{\mu_s}{9}(F_N^{sC} + 8kd) + \frac{8\mu_k}{9}(F_N^{sC} - kd). \quad (7)$$

Now, μ_s is always greater than or equal to μ_k, however, if it is assumed that $\mu_s = \mu_k$, then Eq. (7) can be simplified to:

$$F_T^{sC} = \mu_s F_N^{sC}. \quad (8)$$

Combining equation (5) and (8) gives:

$$\mu_s = F_T^{sC}/F_N^{sC} = F_T^{sO}/(F_N^{sO} - kd), \quad (9)$$

meaning, if k and d are known, and the gross tangential and normal force are measured at the moment of slip of the outer pillars (F_T^{sO} and F_N^{sO}, respectively), it is possible to predict the ratio of gross tangential-to-normal force at which the central pillar will slip; that is, it is possible to estimate the coefficient of static friction by sensing when the outer pillars slip and then examining the forces at that time.

In this simplified mechanical model of the PapillArray, μ_s can be estimated whenever a pillar slips. However, the model makes a number of assumptions which may lead to an underestimate of μ_s. The pillars are assumed not to bend; if they bend, the compressive force they are under will change, and this change is likely to be asymmetric between central and outer pillars, leading to change in normal force distribution across the pillar array. The model assumes that the tangential force is carried equally by all pillars before the outer pillars slip, but this is obviously not true as the pillars have different dimensions and are under different stresses which will likely lead to an asymmetry between tangential forces generated by the central and outer pillars as they bend. It is also assumed that μ_s is constant, i.e., μ_s is assumed to be the same for each pillar; however, there is an observed dependence of μ_s on normal force, and the normal force experienced by the central pillar differs to that of the outer pillars. Finally, in order to further simplify the model, and in the case of just two pillar heights, to reduce the number of unknowns (Eq (7)) and enable the estimate of μ_s, it is assumed that $\mu_k = \mu_s$, however, this has not been confirmed experimentally. This assumption may also contribute to an underestimate of μ_s. However, this underestimation bias is acceptable in a gripping application, as the object will be measured as being slightly more slippery than it truly is, further improving the grip security.

2.3 Prototype design and fabrication

The optimal pillar shape, diameter, number and relative heights of the PapillArray have yet to be determined. In the proof-of-concept prototype that was tested in this work, the diameter of the base

of the PapillArray sensor (from which the pillars emanate) D_{total} = 80 mm with a thickness of 3mm, and each of the cylindrical pillars had a diameter of D = 10 mm and a hemispherical ending, with approximately 15 mm centre to centre spacing. Hemispherical ends were chosen, as flat ends with sharp edges would cause large compressive forces to grow on the edge of the pillar contact area before it would slip. In this embodiment of the PapillArray sensor (as with the simple model above), eight outer pillars surround a single central pillar, in a 3 x 3 grid arrangement. The height of the central pillar was l_C = 15 mm, and the height of outer pillars was l_O = 14 mm; i.e., the height difference between the central pillar and the outer pillars is d = 1 mm. To fabricate this prototype, silicone was cast into a 3D printed ABS plastic mould.

The mould was printed in ABS*plus*® thermoplastic using a Mojo 3D Printer (Stratasys, MN, USA). To smooth the 3D print lines on the surface of the mould, it was suspended over an acetone vapour bath for 3 hours at room temperature. Figure 2A and 2B show the mould before and after the acetone vapour bath, respectively.

PinkySil® (Barnes Products, Sydney, Australia) – a two-component, skin-safe silicone with low viscosity for easy flowing, and short curing period – was used as the material for the prototype. The two components were mixed in equal parts as per the manufacturer instructions and the casting was performed in a single pouring. Degassing procedures were not required, however the silicone was poured from a height to allow better control of the pouring stream, and the mould was shaken gently to remove any bubbles present in the silicone. The silicone was de-moulded after curing (see Figure 2C–2E).

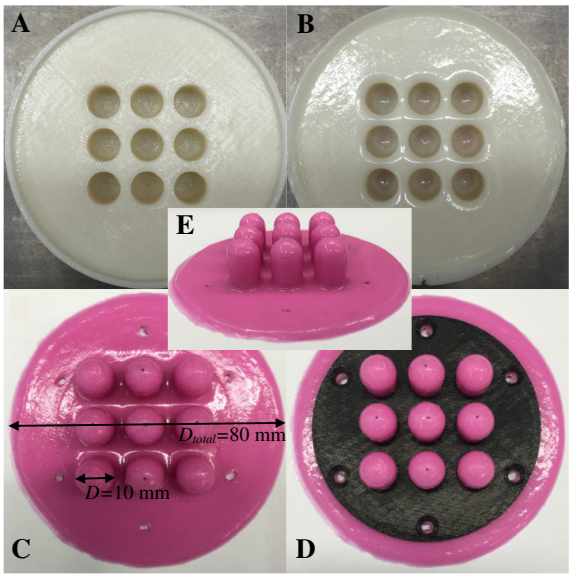

Figure 2. Fabrication of PapillArray prototype. ABS mould A) before and B) after acetone vapour bath; C) silicone prototype, top view; D) prototype with mounting support; E) silicone prototype, side view.

2.4 Prototype validation

To validate the operation of the PapillArray prototype, a number of experiments were performed to apply normal and tangential forces to the PapillArray prototype. To perform these test procedures, a test rig was used, comprising of an XYZ-stage, a 3D force/torque sensor, the PapillArray prototype, a transparent acrylic surface, and a camera. The test rig and test procedures are described below.

2.4.1 Test rig

An XYZ-stage (see Figure 3A) consisting of three translation stages (M-605.1DD, Physik Instrumente (PI) GmbH & Co. KG, Karlsruhe, Germany) was used to bring a transparent acrylic surface into contact with the PapillArray prototype and then shear the acrylic surface across the surface of the PapillArray prototype. Each of the stages have a travel range of 25 mm with a

maximum velocity of 50 mm.s^{-1}, and accuracy of 0.1 µm with step sizes down to 0.3 µm. Compressing of the PapillArray produces a normal force acting on the pillars and shearing of the surface while in contact with the PapillArray produces tangential forces on each of the pillars.

A 3D force/torque sensor (Mini40, SI-80-4, ATI Industrial Automation, Apex, NC, USA) was mounted between the PapillArray prototype and a support frame (see Figure 3D). The forces and torques acting on the PapillArray prototype were sampled at 1 kHz with a PowerLab 16/35 data acquisition unit (AD Instruments, Bella Vista, NSW, Australia).

Video of the PapillArray prototype in contact with the transparent acrylic surface was captured with the native video recording app of a 16GB iPhone 6 (model A1586). The iPhone was placed on a platform (see Figure 3E) such that the PapillArray pillars are viewed through the transparent acrylic surface from (approximately 100 mm) directly below with the center pillar positioned in the middle of the image. The iPhone was connected to a MacBook Pro running QuickTime Player 10.4 to record the iPhone screen in .MOV format with 1334 x 750 pixel resolution at 59.97 fps (frames.s^{-1}). Camera calibration was performed using the MATLAB (R2014b, Mathworks, Natick, MA, USA) Camera Calibration App. The lens distortion coefficients (radial and tangential) were calculated and at the edges of the PapillArray sensor (beyond the maximum deflection of any of the pillars) the distortion was no greater than 1.1 pixels, which corresponds to approximately 0.12 mm. By comparison, the tracking dots on the pillars measure approximately 5 pixels in diameter. Since this distortion has the effect of biasing the measurement of pillar deflection, the effect on the results is only to change the time point at which the pillars are determined to have slipped relative to the stage; however, determining this event time is much more dependent on the slip detection rule used (see section *2.4.3.2 Slip detection*).

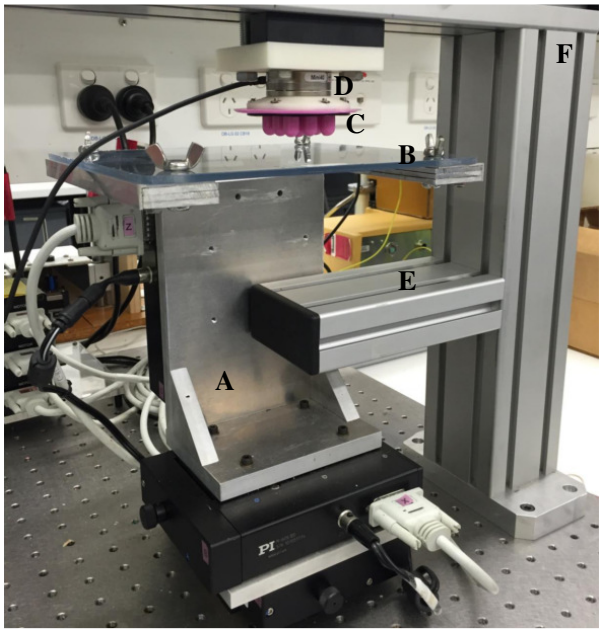

Figure 3. Test rig. A) XYZ-stage, B) acrylic surface, C) PapillArray prototype, D) 3D force/torque sensor, E) platform for video capture, and F) support frame.

A small hole was created with a pin at the central point of the selected pillars, which was filled with black ink to form a reliable marker for tracking during video analysis. Furthermore, a black and white checkerboard pattern comprising of a row of three 10 mm squares was attached to the acrylic surface to provide a reference point for tracking the position of the surface as well as to provide a reference for the spatial unit conversion (pixels to mm).

2.4.2 Test procedures

2.4.2.1 XYZ-stage protocol

The XYZ-stage is programmed to move vertically towards the PapillArray prototype to a predetermined position that results in the desired normal force (0.5 N for measuring μ_s, and 5, 7.5, 10, 12.5 and 15 N for analysing the pillar slipping behaviour – see below) at a velocity of 2.5 mm.s^{-1}. The XYZ-stage holds that position for 1.5 s, then moves laterally at a velocity of 2.5 mm.s^{-1} for a total of 15 mm. The stage then moves vertically away from the PapillArray prototype back to the starting height, thus unloading the forces, then moves laterally to return to the starting position.

2.4.2.2 Characterising the spring constant

By recording the XYZ-stage position that results in the desired normal force (5, 7.5, 10, 12.5, and 15 N), the spring constant can be calculated according to Hooke's Law. Since, at these normal force levels, all nine of the PapillArray sensor pillars are compressed against the acrylic surface, the spring constant k is equal to 1/9th of the gradient of the line defined by stage position versus normal force.

2.4.2.3 Measuring friction

To ensure that the three surfaces used for testing had different values of μ_s and that the μ_s of each surface remained consistent throughout the testing, it was necessary to measure the μ_s. The μ_s was measured by performing the protocol above at a normal force of 0.5 N – at this normal force, only the central pillar makes contact with the surface. The friction was measured before and after testing the pillar behaviour for each combination of frictional condition and testing normal force (see below).

2.4.2.4 Pillar behaviour

The behaviour of the sensor was tested at five different normal force levels: 5, 7.5, 10, 12.5 and 15 N. The XYZ-stage was programmed to apply the normal and tangential forces as described above. At the same time, the force/torque signals from the ATI sensor were recorded and video was captured of the pillars in contact with acrylic surface.

Three surfaces were used with different frictional properties: (i) acrylic cleaned with ethanol (base friction condition), (ii) acrylic covered in olive oil (low friction condition), and (iii) acrylic coated with a thin layer of soap that has been allowed to dry (high friction condition).

For each combination of normal force (5, 7.5, 10, 12.5 and 15 N) and surface (acrylic: coated with oil, cleaned with alcohol, coated with soap), the following testing was performed: test friction at 0.5 N (once), test pillar behaviour at desired normal force (five times), test friction at 0.5 N (once).

2.4.3 Analysis

2.4.3.1 Pre-processing and data fusion

To remove any high-frequency noise in the force signals, a 2nd-order low-pass Butterworth filter with a cut-off frequency of 10 Hz was applied.

The recorded videos were used to monitor the deflections of the central pillar and one of the eight outer pillars of the PapillArray prototype during lateral movement of the acrylic surface. The Kanade-Lucas-Tomasi algorithm was used to perform point tracking in MATLAB (Mathworks, Natick, MA, USA). Three points were tracked throughout the video recording: (i) the centre of the central pillar, (ii) the centre of one outer pillar – this was chosen as the pillar directly leading the central pillar in the direction of shearing – and (iii) a point on the reference grid (to monitor the position of the acrylic surface).

The result of point-tracking gives the deflection of the central and outer pillars relative to the position of the acrylic surface, and subsequently, relative to the undeflected position of each pillar. A single frame of the video tracking and the pillar deflection is shown in Figure 4. A 5 Hz 2nd-order low-pass Butterworth filter was then applied to remove tracking jitter from the deflection data.

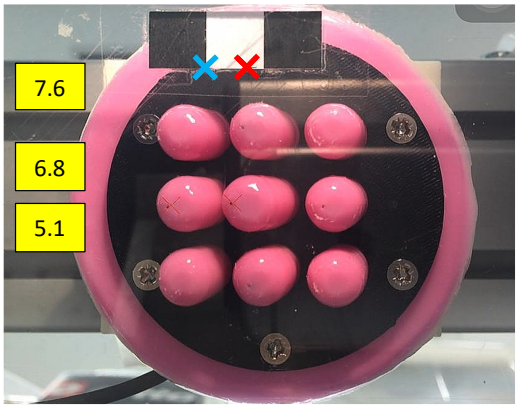

Figure 4. A single frame of video captured during the testing procedure. The red cross is the original position of the marker; the blue cross is the current position of the marker which moves with the acrylic plate. The values highlighted in yellow are the deflections (mm) of the marker (top), the central pillar (middle), and the outer pillar to the left of the central pillar (bottom).

Synchronisation of the filtered force/torque and deflection signals were required since the original data were recorded on two different devices. At the end of each stimulus, the XYZ-stage accelerated in the negative Z-direction (normal to the PapillArray pillars) to retract the acrylic surface away from the PapillArray sensor, in order to unload the normal force. This results in a large acceleration in the measured normal force as well as the calculated central pillar deflection as the tangential bending force is suddenly removed. The large negative peaks in the second derivatives with respect to time of the filtered normal force and the central pillar deflection were used to synchronise the force and deflection data.

2.4.3.2 Slip detection

Ideally, since the stage is moving at a velocity of 2.5 mm.s^{-1}, if the pillar is stuck (not slipping), it too should be deflecting at a velocity of 2.5 mm.s^{-1} at its tip, and when the pillar slips, the deflection velocity should become 0 mm.s^{-1}. This however is not the case in practice and due to bending of the pillar, the pillar first appears to move at the same velocity as the stage, however this velocity decreases slowly as the pillar appears to roll at the contact point. The moment of slip was therefore heuristically determined as the moment when the deflection velocity of the pillar (i.e., the first derivative of the deflection position with respect to time) decreased to 5% of the stage velocity (i.e. when the deflection velocity of the pillar first drops to below 0.125 mm.s^{-1}) – this is close to zero, but above the level of frame-to-frame noise of the pillar deflection velocity. In this work to prove the principle of operation of the PapillArray, this threshold was sufficient for identifying the moment of slip, however, in other real situations the detection algorithm will certainly need to be more complex/robust. In future, each pillar will be instrumented internally to measure its deflection, and the slip event will be less ambiguous.

2.4.3.3 Measuring friction

The ratio of the tangential force to normal force at the moment of slip (as determined by the video analysis) of the central pillar (the only pillar in contact at 0.5 N of normal force) was taken to be an estimate of μ_s.

2.4.3.4 Pillar slip behaviour

The principle of operation of the PapillArray sensor is that the outer (shorter) pillar should slip under a smaller tangential force compared to the central (taller) pillar. To determine whether this is satisfied, the tangential and normal forces at the moment of slip of the outer and central pillars respectively, were determined for comparison. A prediction of $\mu_s = F_T^{sC}/F_N^{sC}$ (Eq. (9)) was also calculated from the measured tangential and normal forces when the outer pillar slips (F_T^{sO} and F_N^{sO}, respectively) and a comparison was made to the measured F_T^{sC}/F_N^{sC} which are measured some time later when the central pillar finally slips.

3. Results

3.1 Characterising the slip constant, k

The stage positions (mm) for each of the normal forces (N) were used to calculate the spring constant, k, of the PapillArray sensor pillars (Figure 5). The equation of the line of best fit and the R^2 value of the fit are shown on the plot. The R^2 value is > 0.99, indicating an excellent fit of the line to the data. The spring constant k, is the gradient of the line of best fit divided the number of pillars: k = 1.174 N/mm.

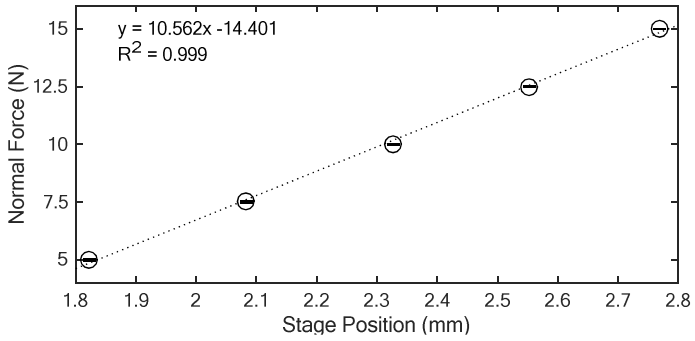

Figure 5. Calculating the spring constant of the silicone. Stage position for each normal force with line of best fit, equation and R^2 value. Markers are the mean values and error bars extend to ± SD.

3.2 Measuring friction

A typical recording of the forces and central pillar deflection during measurement of the μ_s are shown in Figure 6A and 6B, respectively. It was observed that when the acrylic plate begins to shear (at approximately 2.4 s), there is a decrease in the normal force. This is expected as the XYZ-stage is programmed to remain at the same height while shearing the acrylic surface, and the pillars of the PapillArray sensor bend, meaning that the effective height of the sensor decreases slightly. The μ_s was taken as the ratio of tangential force to normal force at the moment the central pillar slips (indicated with the rightmost solid vertical line).

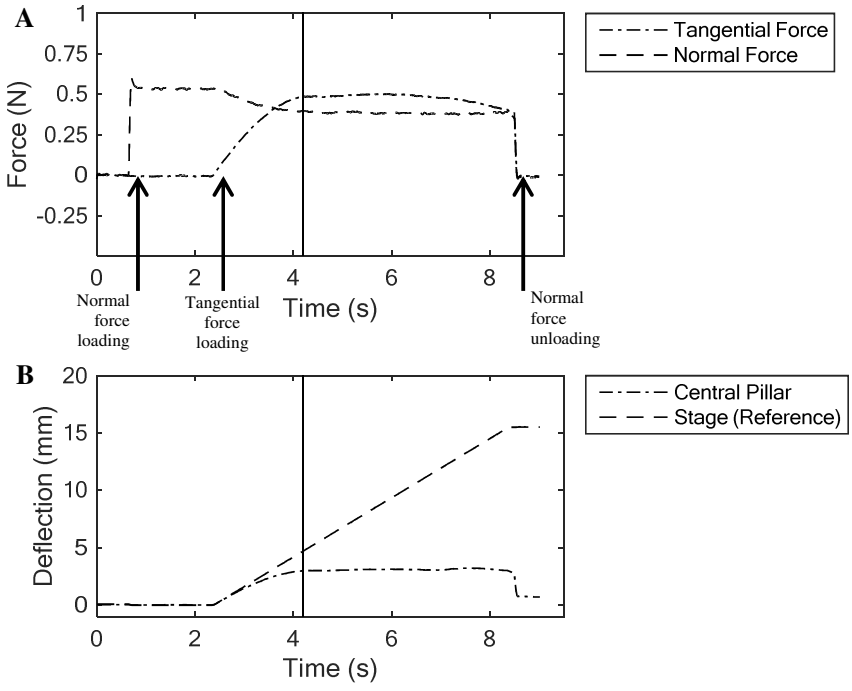

Figure 6. A) Force and B) pillar deflection data used for friction calculation – High friction surface, after 5 N test. Moment of slip of central pillar is indicated by solid vertical line.

The measured μ_s, before and after each of the frictional testing conditions, are reported in Table 1. The mean ± SD of the low, base and high friction surfaces were 0.234 ± 0.045, 0.959 ± 0.020 and 1.238 ± 0.029, respectively. The small standard deviations indicate that the μ_s was relatively stable throughout the testing for each of the surfaces.

Table 1. Coefficient of static friction, μ_s (measured at 0.5 N with only central pillar in contact) before and after testing at each normal force level with each of the surface frictional conditions.

	μ_s		
Test	Low Friction	Base Friction	High Friction
Before 5 N	0.219	0.926	1.278
After 5 N	0.317	0.963	1.224
Before 7.5 N	0.181	0.952	1.191
After 7.5 N	0.262	0.966	1.267
Before 10 N	0.195	0.979	1.213
After 10 N	0.244	0.993	1.265
Before 12.5 N	0.183	0.957	1.216
After 12.5 N	0.263	0.960	1.250
Before 15 N	0.201	0.934	1.219
After 15 N	0.272	0.957	1.262
Mean	**0.234**	**0.959**	**1.238**
SD	**0.045**	**0.020**	**0.029**

3.3 Pillar slip behaviour

A typical recording of the forces and pillar deflections during the testing of the pillar behaviour are shown in Figure 7A and 7B, respectively. The moment of slip of the outer pillar (indicated by the left-most solid vertical line) occurs at a lower tangential-to-normal force ratio than the moment of slip of the central pillar (indicated by the rightmost solid vertical line).

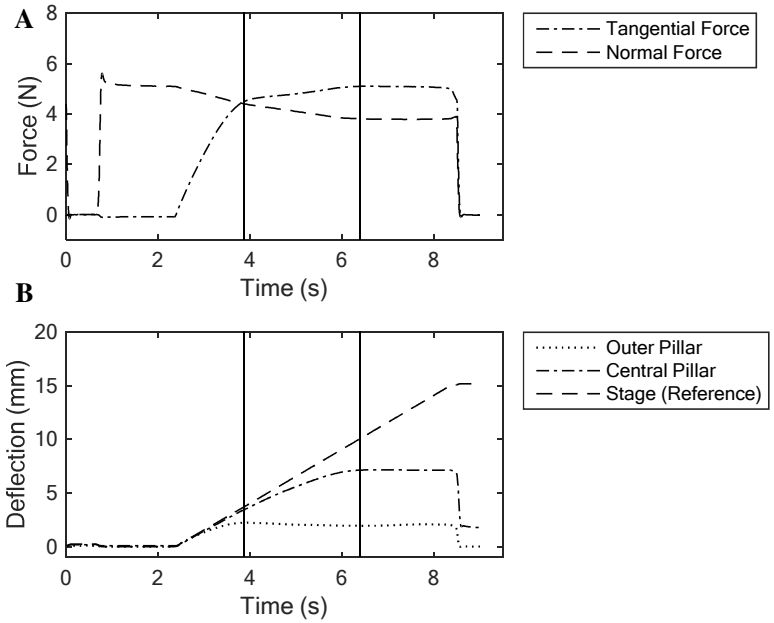

Figure 7. A) Force and B) pillar deflection data used for testing pillar slip behaviour – high friction surface (acrylic treated with dried soap), 5 N normal force level, 4th repetition. Moment of slip is indicated by solid vertical line – left-most vertical line for outer pillar, right-most vertical line for central pillar.

For the high and base friction surfaces, as expected, the moment of slip of the outer pillar occurs at a lower tangential-to-normal force ratio than the moment of slip of the central pillar in all cases.

This can be seen in Figure 8A and 8B, respectively. For the low friction surface (acrylic coated with olive oil) this same behaviour was observed only at a normal force of 15 N; for smaller normal forces, both pillars were observed to slip at approximately the same tangential to normal force ratio (Figure 8 C). The reason for this behaviour is not immediately clear; however, it is suspected that this is related to the observed dependency of μ_s on the normal force. This may be indicative of a limitation of the PapillArray sensor's range of operation for μ_s.

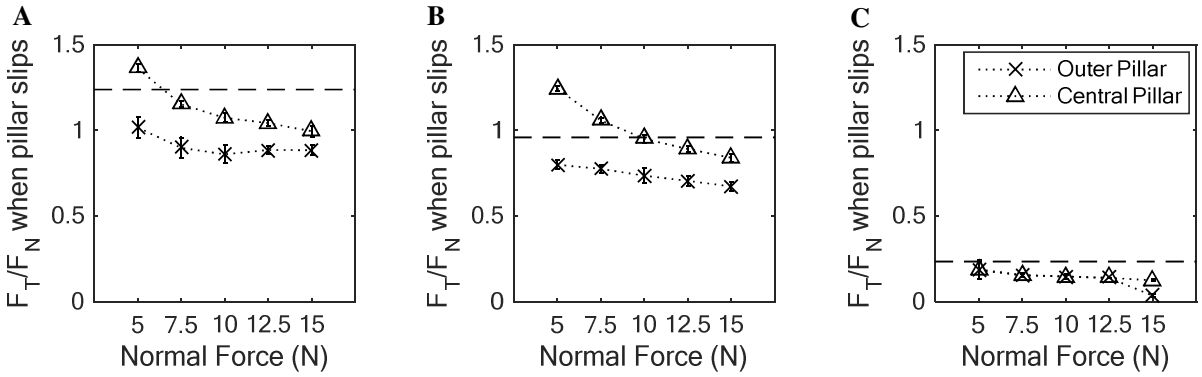

Figure 8. Tangential-to-normal force ratio at which each pillar slips at each normal force level for the A) high, B) base, and C) low friction surfaces. Markers are the mean values and error bars extend to ± SD. Dashed horizontal line indicates μ_s measured at 0.5 N normal force.

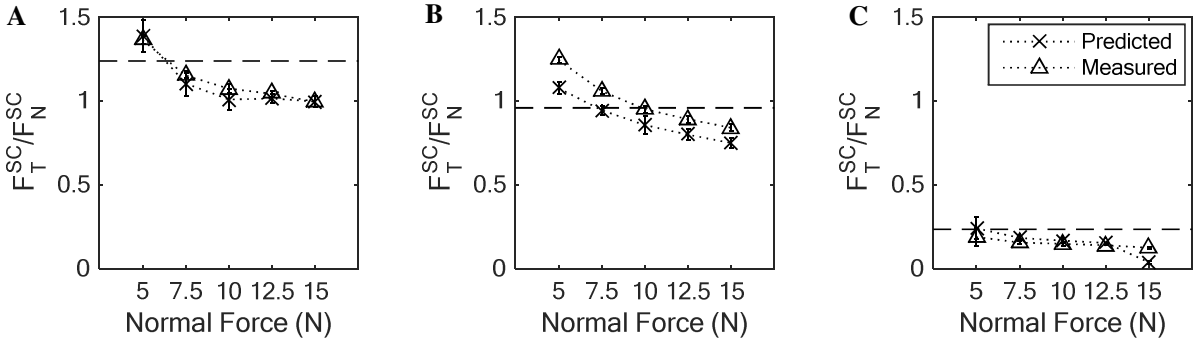

Figure 9. Actual and predicted F_T^{SC}/F_N^{SC} for each normal force level for the A) high, B) base, and C) low friction surfaces. Markers are the mean values and error bars extend to ± SD. Dashed horizontal line indicates μ_s measured at 0.5 N normal force.

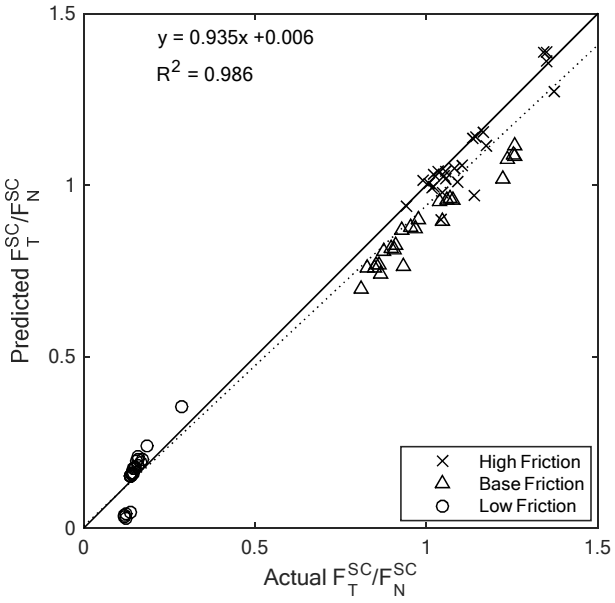

Figure 10. Actual and predicted ratio $F_T^{sC}/F_N^{sC} = F_T^{sO}/\left(F_N^{sO} - kd\right)$ with line of best fit, equation and R^2 value.

Based on the measured tangential and normal force when the outer pillar slips, the ratio F_T^{sC}/F_N^{sC} was predicted using Eq. (9). The predicted and measured F_T^{sC}/F_N^{sC} are shown in Figure 9 for each normal force and frictional surface. For the high and base frictions, the predicted ratio is slightly underestimated. A scatter plot of the predicted and measured ratios is also presented in Figure 10. The equation and R^2 value for a line of best fit are also shown. The R^2 value is greater than 0.98 indicating a good fit, and the gradient of the line is 0.935, which indicates that the predicted value is a slight underestimate of the ratio, as can be observed in Figure 10. This underestimate could be due to a number of assumptions made in the simplified model (as discussed in section *2.2 A simplified mechanical model*).

4. Discussion

In this work, the proof-of-concept design and prototype evaluation of a grip security sensor – the PapillArray sensor – has been presented. The PapillArray sensor detects incipient slip while the grip is still secured, which can enable force modulation before total loss of grip is experienced. Unlike the incipient slip sensors in the literature, the PapillArray is purposely designed to encourage incipient slip on the periphery first, where the local grip force (and hence traction) is smallest – pillars of different heights create a non-uniform pressure distribution when the sensor is in contact with a surface (akin to the curved surface of the human finger), and individual sections of the sensor are able to move independently of each other (just as the fingerprint allows somewhat independent movement of sections of the human fingerpad).

A simplified mathematical formulation of the forces acting on one embodiment of the PapillArray has been described and a prototype has been made and tested under different normal forces and frictional conditions.

The following sections contain a discussion of the utility of the sensor, design considerations as well as considerations for instrumentation and miniaturization of the PapillArray sensor.

4.1 Utility of the PapillArray

Both with and without continuous normal and tangential force monitoring, the PapillArray sensor could be used to improve dexterous manipulation in robotic and prosthetic grippers. Without continuous monitoring of F_N and F_T, the rate at which warnings are signalled as well as the number of warnings could still indicate the urgency with which corrective action is required as well as the magnitude of the corrective action. However, with continuous force monitoring, it may be possible

to also determine μ_s, and grip corrections would be more informed; it would be very difficult to adequately adjust the grip force without measuring this same grip force, and the weight of the object, and the friction.

For maximum utility, the PapillArray sensor requires planar contact with a surface – if the surface is not planar, the relative compression of each pillar cannot be known unless the compressive stress on each pillar is measured independently. For example, for a convex surface, the force on the outer pillars will be less than they are estimated to be using the model suggested herein, causing them to slip at a smaller tangential force, leading to an underestimation of the coefficient of friction and hence excessive grip force corrections; but here the object is more likely to be crushed than dropped. Miniaturisation of the PapillArray, is one way of ensuring planar contact, at least over certain length scales. However, non-planar contact does not render the PapillArray sensor useless – it is highly improbable that the PapillArray sensor will come into contact with an object in such an orientation that would exactly compliment the height distribution of the pillars, therefore, each pillar will still experience a different normal force, and as such, the PapillArray will issue a warning when the least-compressed pillar slips.

4.2 PapillArray design considerations

A number of physical design features of the PapillArray have yet to be optimised including pillar shape, diameter, number and relative heights.

The pillars are designed with rounded ends, as flat ends with sharp edges would cause large compressive forces to grow on the edge of the pillar contact area before it would slip. Currently, hemispherical ends are used, but it has been observed that as the experimental stage moves laterally with a fixed height, this leads to a decompression of the pillar as it bends. An intermediate geometry between flat and spherical might better maintain the expected distribution of normal force across the pillars as they bend.

The diameter of the pillars may also need to be optimised. A larger diameter would reduce the bending of the pillars, however it would also increase the amount of normal force required to compress the pillars. Furthermore, the diameter need not be the same for all pillars as there may be a benefit, with respect to gripping, in having outer pillars with a smaller/larger diameter than the inner pillars so as to take advantage of the bending properties.

The optimal number of pillars and the ideal distribution of pillar heights are yet to be determined. With more pillars and more height differences, a larger range of frictions and normal forces could be accommodated for, and a series of warnings could be given to prevent loss of the object as the tangential force increases. The rate at which warnings are signalled as well as the number of warnings could indicate the urgency with which corrective action is required. Furthermore, with each warning, more information about the contact interface can be learned.

4.3 Instrumentation and miniaturisation

A method of instrumenting each of the pillars of the PapillArray sensor is required to record the pillar deflection, continuously. Absolute pillar deflection relative to the undeflected pillar position can indicate whether a pillar is stuck or slipping, however, more information could be gained by looking at the patterns of pillar deflection across the entire PapillArray sensor. For example, observing the pillar deflections in two dimensions and the relative deflections of all the pillars with respect to each other may indicate the load force direction, as well as the presence of any torque.

Miniaturisation issues would also need to be considered when choosing a method of instrumentation, as the PapillArray sensor is required to have many pillars, yet still fit on a finger of a robotic gripper. Real-time analysis of the deflection signals is also required to indicate when a pillar begins to slip during a manipulation task.

5. Conclusions

In this work, the principle of operation of one embodiment of the PapillArray sensor has been validated by using video point tracking to measure the deflection of the pillars of the sensor. A comparison was also made to a simplified mechanical model of the prototype with compressible but unbending pillars. Using this model, a prediction of the tangential-to-normal force ratio at the moment of slip of the central pillar was also made. The ideal embodiment of the PapillArray sensor is yet to be determined, and a method of instrumentation is required to measure the deflection of individual pillars in real-time, however, the utility of the PapillArray sensor as an indicator of grip security (and which could also be used to estimate μ_s) for improved dexterous manipulation of prosthetic and robotic grippers is undeniable.

Acknowledgements

This work was supported in part by an Australian Research Council Future Fellowships Grant [grant number FT130100858].

References

[1] Å. B. Vallbo and R. Johansson, "Properties of cutaneous mechanoreceptors in the human hand related to touch sensation," *Human Neurobiology,* vol. 3, pp. 3-14, 1984.
[2] P. Jenmalm, I. Birznieks, A. W. Goodwin, and R. S. Johansson, "Influence of object shape on responses of human tactile afferents under conditions characteristic of manipulation," *European Journal of Neuroscience,* vol. 18, pp. 164-176, 2003.
[3] H. Khamis, S. J. Redmond, V. Macefield, and I. Birznieks, "Classification of texture and frictional condition at initial contact by tactile afferent responses," in *International Conference on Human Haptic Sensing and Touch Enabled Computer Applications*, 2014, pp. 460-468.
[4] M. I. Tiwana, S. J. Redmond, and N. H. Lovell, "A review of tactile sensing technologies with applications in biomedical engineering," *Sensors and Actuators A: Physical,* vol. 179, pp. 17-31, 2012.
[5] R. Fernandez, I. Payo, A. S. Vazquez, and J. Becedas, "Micro-vibration-based slip detection in tactile force sensors," *Sensors,* vol. 14, pp. 709-730, 2014.
[6] B. Choi, H. R. Choi, and S. Kang, "Development of tactile sensor for detecting contact force and slip," in *IEEE/RSJ International Conference on Intelligent Robots and Systems*, 2005, pp. 2638-2643.
[7] Z. Su, K. Hausman, Y. Chebotar, A. Molchanov, G. E. Loeb, G. S. Sukhatme*, et al.*, "Force estimation and slip detection/classification for grip control using a biomimetic tactile sensor," in *Proceedings of IEEE-RAS 15th International Conference on Humanoid Robots (Humanoids)*, 2015, pp. 297-303.
[8] T. Maeno, T. Kawamura, and S.-C. Cheng, "Friction estimation by pressing an elastic finger-shaped sensor against a surface," *IEEE Transactions on Robotics and Automation,* vol. 20, pp. 222-228, 2004.
[9] K. Nakamura and H. Shinoda, "Tactile sensing device instantaneously evaluating friction coefficients," in *Technical Digest of the Sensor Symposium*, 2001, pp. 151-154.
[10] W. Chen, H. Wen, H. Khamis, and S. J. Redmond, "An eight-legged tactile sensor to estimate coefficient of static friction: Improvements in design and evaluation," in *International Conference on Human Haptic Sensing and Touch Enabled Computer Applications*, 2016, pp. 493-502.
[11] R. S. Johansson and G. Westling, "Signals in tactile afferents from the fingers eliciting adaptive motor responses during precision grip," *Experimental Brain Research,* vol. 66, pp. 141-154, 1987.
[12] M. T. Francomano, D. Accoto, and E. Guglielmelli, "Artificial sense of slip: A review," *IEEE Sensors Journal,* vol. 13, pp. 2489-2498, 2013.
[13] S. Ando and H. Shinoda, "Ultrasonic emission tactile sensing," *IEEE Control Systems,* vol. 15, pp. 61-69, 1995.
[14] G. Canepa, R. Petrigliano, M. Campanella, and D. De Rossi, "Detection of incipient object slippage by skin-like sensing and neural network processing," *IEEE Transactions on Systems, Man, and Cybernetics, Part B: Cybernetics,* vol. 28, pp. 348-356, 1998.
[15] T. Maeno, T. Kawai, and K. Kobayashi, "Analysis and design of a tactile sensor detecting strain distribution inside an elastic finger," in *Proceedings of IEEE/RSJ International Conference on Intelligent Robots and Systems*, 1998, pp. 1658-1663.
[16] T. Maeno, K. Kobayashi, and N. Yamazaki, "Sensing mechanism of the partial incipient slip at the surface of cylindrical fingers during the precision grip," in *Proceedings of ASME Summer Bioengineering Conference*, 1997, pp. 117-118.
[17] T. Maeno, S. Hiromitsu, and T. Kawai, "Control of grasping force by detecting stick/slip distribution at the curved surface of an elastic finger," in *Proceedings of IEEE International Conference on Robotics and Automation*, 2000, pp. 3895-3900.

[18] I. Fujimoto, Y. Yamada, T. Morizono, Y. Umetani, and T. Maeno, "Development of artificial finger skin to detect incipient slip for realization of static friction sensation," in *Proceedings of IEEE International Conference on Multisensor Fusion and Integration for Intelligent Systems*, 2003, pp. 15-20.
[19] Y. Tada and K. Hosoda, "Acquisition of multi-modal expression of slip through pick-up experiences," *Advanced Robotics,* vol. 21, pp. 601-617, 2007.
[20] S. Shirafuji and K. Hosoda, "Detection and prevention of slip using sensors with different properties embedded in elastic artificial skin on the basis of previous experience," *Robotics and Autonomous Systems,* vol. 62, pp. 46-52, 2014.
[21] L. Marconi and C. Melchiorri, "Incipient slip detection and control using a rubber-based tactile sensor," in *Proceedings of IFAC World Congress*, 1996, pp. 475-480.
[22] E. Holweg, H. Hoeve, W. Jongkind, L. Marconi, C. Melchiorri, and C. Bonivento, "Slip detection by tactile sensors: algorithms and experimental results," in *Proceedings of IEEE International Conference on Robotics and Automation*, 1996, pp. 3234-3239.
[23] H. William, Y. Ibrahim, and B. Richardson, "A tactile sensor for incipient slip detection," *International Journal of Optomechatronics,* vol. 1, pp. 46-62, 2007.
[24] A. Ikeda, Y. Kurita, J. Ueda, Y. Matsumoto, and T. Ogasawara, "Grip force control for an elastic finger using vision-based incipient slip feedback," in *Proceedings of IEEE/RSJ International Conference on Intelligent Robots and Systems*, 2004, pp. 810-815.
[25] J. Ueda, A. Ikeda, and T. Ogasawara, "Grip-force control of an elastic object by vision-based slip-margin feedback during the incipient slip," *IEEE Transactions on Robotics,* vol. 21, pp. 1139-1147, 2005.
[26] N. Watanabe and G. Obinata, "Grip force control based on the degree of slippage using optical tactile sensor," in *Proceedings of International Symposium on Micro-NanoMechatronics and Human Science*, 2007, pp. 466-471.
[27] Y. Ito, K. Youngwoo, and G. Obinata, "Robust slippage degree estimation based on reference update of vision-based tactile sensor," *Sensors Journal, IEEE,* vol. 11, pp. 2037-2047, 2011.
[28] A. Mamun and M. Y. Ibrahim, "New approach to detection of incipient slip using inductive sensory system," in *IEEE International Symposium on Industrial Electronics*, 2010, pp. 1901-1906.
[29] W. Yuan, R. Li, M. A. Srinivasan, and E. H. Adelson, "Measurement of shear and slip with a GelSight tactile sensor," in *Proceedings of IEEE International Conference on Robotics and Automation*, 2015, pp. 304-311.
[30] M. R. Tremblay and M. R. Cutkosky, "Estimating friction using incipient slip sensing during a manipulation task," in *Proceedings of IEEE International Conference on Robotics and Automation*, 1993, pp. 429-434.